Article

Controlled Aggregation of ME$_4^-$ Binary Anions (M = Cr, Mo; E = As, Sb) into One-Dimensional Arrays: Structures, Magnetism and Spectroscopy

Banu Kesanli, James Fettinger, and Bryan Eichhorn

J. Am. Chem. Soc., **2003**, 125 (24), 7367-7376• DOI: 10.1021/ja034207e • Publication Date (Web): 21 May 2003

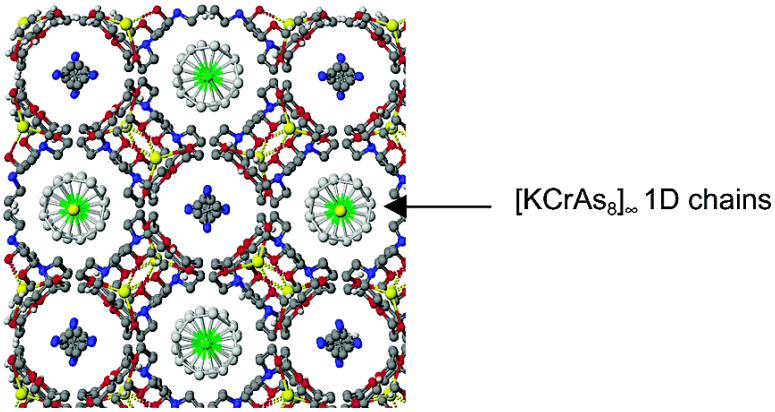

More About This Article

Additional resources and features associated with this article are available within the HTML version:

- Supporting Information
- Links to the 2 articles that cite this article, as of the time of this article download
- Access to high resolution figures
- Links to articles and content related to this article
- Copyright permission to reproduce figures and/or text from this article

View the Full Text HTML

J|A|C|S
ARTICLES
Published on Web 05/21/2003

Controlled Aggregation of ME_8^{n-} Binary Anions (M = Cr, Mo; E = As, Sb) into One-Dimensional Arrays: Structures, Magnetism and Spectroscopy

Banu Kesanli, James Fettinger, and Bryan Eichhorn*

Contribution from the Department of Chemistry and Biochemistry, University of Maryland, College Park, Maryland 20742

Received January 16, 2003; E-mail: eichhorn@umd.edu

Abstract: The $[ME_8]^{n-}$ ions where M = Cr, Mo; E = As, Sb; n = 2, 3 have been prepared from the corresponding E_7^{3-} Zintl ions and M(naphthalene)$_2$ precursors. The complexes and their $[A(crypt)]^+$ salts (A = Na, K) are formed in 20−45% crystalline yields and have been characterized by UV−vis spectroscopy, EPR, cyclic voltammetry, magnetic susceptibility, electrospray mass spectrometry (ESI−MS) and single-crystal X-ray diffraction. The structures are defined by crown-like cyclo-E_8 rings that are centered by transition metals. $MoAs_8^{2-}$ (**2**) is a 16 e^- diamagnetic complex whereas $MoSb_8^{3-}$ (**5**) and the $CrAs_8^{3-}$ salts (**3** and **4**) are 17 e^- paramagnetic complexes. The ESI-MS spectra show free and alkali-complexed ME_8^{n-} ions. The K^+ salt of $CrAs_8^{3-}$ (**4**) crystallizes in a one-dimensional chain structure of $[KCrAs_8]^{2-}$ repeat units whereas the Na^+ salt (**3**) as well as **2** and **5** crystallize in "free ion" structures. The Cr atoms in **3** and **4** are formally d^1 Cr^{5+} centers that show EPR signals at g = 2.001 with small As hyperfine interactions of 3.6 G. The susceptibility of the $[KCrAs_8]^{2-}$ salt **4** was modeled as a 1D Heisenberg antiferromagnet with a small $-J/k_B$ of 3K arising from antiferromagnetic couplings of the d^1 centers whereas **3** shows Curie−Weiss behavior. The electrochemical studies show metal-based oxidations for **3**−**5** but a ligand based oxidation for **2**. The electronic spectra are interpreted in terms of the molecular orbital analysis of Li and Wu. The differences in formal oxidation states of the metals is described in terms of a Zintl−Klemm formalism involving E_8^{8-} rings that are isoelectronic to S_8. The factors governing the formation of 1D chains versus free ions are presented.

Introduction

The ability to control the aggregation of molecular subunits into nano and microscopic arrays is a central feature in supramolecular chemistry and molecular based nanoscience. Assembled organic aggregates often rely on large numbers of weak intermolecular forces (e.g., hydrogen bonds) that provide structural integrity yet allow for reversible binding.[1] Inorganic aggregates primarily utilize metal−ligand coordinate bonds to form supramolecular arrays and coordination polymers.[2,3] The remarkable 1D $[RbNbAs_8]^{2-}$ (**1**) polymer chain reported by von Schnering and co-workers is a unique example of a carbon-free transition metal main group coordination polymer.[4] The As_8 unit in **1** has a crown-like structure with an interstitial Nb atom. The $NbAs_8^{3-}$ ions are linked into a one-dimensional chain by coordinating to Rb^+ ions (see I). According to the Zintl−Klemm formalism,[5,6] the As_8 ring possesses a −8 charge which formally requires Nb to be in the +5 oxidation state. We subsequently reported[7] a "free-ion" As_8 complex, $[MoAs_8]^{2-}$ (**2**), which is the Mo analogue of the subunit in **1** and was prepared from the As_7^{3-} Zintl ion (see II). In contrast to **1**, all of the alkali ions in this complex are encapsulated in 2,2,2-crypt counterions and are well separated from the binary anions. Complex **2** also has a regular crown-like As_8 ring with a transition metal in the center. The gas-phase studies of **2** show that it preferentially binds to larger alkali ions.[7] Detailed theoretical studies by Li and Wu[8] gave further insight into the structure and bonding of these unusual type of ions. Their studies

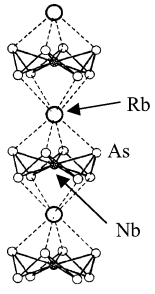

I

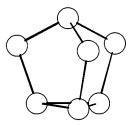

II

(1) Reinhoudt, D. N.; Crego-Calama, M. *Science* **2002**, *295*, 2403.
(2) Ikkala, O.; Brinke, G. T. *Science* **2002**, *295*, 2407.
(3) Schubert, U. S.; Eschbaumer, C. *Angew. Chem., Int. Ed. Engl.* **2002**, *41*, 2892.
(4) von Schnering, H.-G.; Wolf, J.; Weber, D.; Ramirez, R.; Meyer, T. *Angew. Chem., Int. Ed. Engl.* **1986**, *25*, 353.
(5) Zintl, E. *Angew. Chem.* **1939**, *52*, 1.
(6) Klemm, W. *Proc. Chem. Soc.* **1958**, 329.
(7) Eichhorn, B. W.; Mattamana, S. P.; Gardner, D. R.; Fettinger, J. C. *J. Am. Chem. Soc.* **1998**, *120*, 9708.
(8) Li, J.; Wu, K. *Inorg. Chem.* **2000**, *39*, 1538.

also suggested that it is feasible to synthesize different derivatives of the cyclic polyarsenides, which are all predicted to be diamagnetic.

Polyarsenic ring systems can be categorized as either alkyl arsines[9−12] that include *t*-Bu_6As_8, $(RAs)_n$ where $n = 3-6$ and/or bare arsenic rings,[13−17] As_n. The reactivity of alkylarsines with transition metal centers involves ring expansion or retention as well as loss of the R group to give naked As atom species. The modifications are often dictated by the sterics and electronics of the transition metal fragment.[9] A variety of complexes are formed with alkylarsines include $(RAs)_8$ containing compounds such as $Mo_2(CO)_6[\mu\text{-}\eta^4\text{-}catena\text{-}(RAs)_8]$ where R = Me, *n*-Pr, Ph.[11,18] Scherer described a bare As_8 ring system in the $[(Cp"Nb)_2(\mu,\eta^{4:4}-As_8)]$ compound.[16] This ring has a distorted cyclooctatetraene-like structure with capping NbCp" units. In contrast to complexes **1** and **2**, the As_8 units of the organometallic compounds are formally neutral moieties.

In comparison, the organo-antimony complexes and their transition metal derivatives are much less developed than the corresponding As chemistry. Cyclic organostibanes $(RSb)_n$ can be prepared where $n = 3$, 4, 5 and 6[19−22] and Breunig et al.[23,24] described the synthesis of polycyclic R_4Sb_8 complexes. For example, $(C_6H_5Sb)_6\cdot(1,4\text{-dioxane})$[25] contains an Sb_6 ring in a chair confirmation with the phenyl groups in equatorial positions. Naked Sb clusters are also known, such as the Sb_7^{3-} Zintl ion,[26,27] which changes in structure from nortricyclane-like to norbornadiene-like in the $[Sb_7M(CO)_3]^{3-}$ type complexes, (M = Cr, Mo, W).[28,29]

During the course of our investigations of incorporating bare metal atoms into E_7^{3-} Zintl ions, we found that the $M(arene)_2$ (M = Mo, arene = Me-naphthalene; M = Cr, arene = naphthalene) precursors produced *cyclo*-E_8 ring compounds (E = As, Sb). These reactions have developed into convenient routes to a growing number of ME_8^{n-} ions. Goals in this program include the following: (1) developing a general synthesis for the $[ME_8]^{n-}$ type ions; (2) controlling the assembly of these ions into ordered arrays; (3) investigating the properties of the "free ions" and ordered arrays; and (4) studying their utility as precursors to binary solids. Herein, we report the synthesis and characterization of complexes with a general formula of ME_8^{n-} (where M = Cr, Mo; E = As, Sb and n = 2, 3) including rare examples of paramagnetic transition metal Zintl ion complexes. The factors governing the formation of diamagnetic d^0 and paramagnetic d^1 systems are described. In addition, the parameters that discriminate between the formation of isolated ME_8^{n-} ions versus $[AME_8]^{n-}$ one-dimensional (1D) chains (A = alkali ion) are presented. The preliminary study on $MoAs_8^{2-}$ has been reported.[7]

Scheme 1

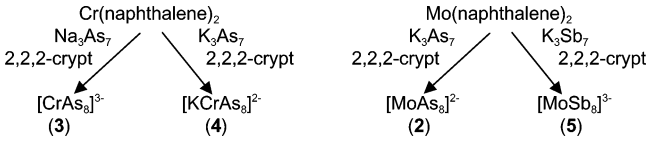

Results

Synthesis. Toluene solutions of $M(arene)_2$ (M = Mo, arene = Me-naphthalene, naphthalene; M = Cr, arene = naphthalene) react with ethylenediamine (en) solutions of A_3E_7 (A = Na, K; E = As, Sb) in the presence of 2,2,2-crypt to give the respective $[Na(2,2,2\text{-crypt})]^+$ or $[K(2,2,2\text{-crypt})]^+$ salts of the $[ME_8]^{n-}$ ions. The formula and the numbering of these complexes are summarized in Scheme 1. Complex **4**, $[KCrAs_8]^{2-}$, crystallizes in a 1D chain structure, whereas the others crystallize as isolated anions in the solid state. The reactions do not occur in the absence of 2,2,2-crypt, which is common in the synthesis of metalated Zintl complexes (e.g., $[E_7M(CO)_3]^{3-}$).[28] The mechanism of formation of the ME_8^{n-} ions from the E_7^{3-} precursors is still unclear at present (see discussion), however, this synthetic method provides a very convenient, reproducible, relatively high yield route to the $[ME_8]^{n-}$ complexes.

The four ME_8^{n-} complexes crystallize from solution in reasonable to good yields (20−45%) with different crystal symmetries and various degrees of solvation (see the next section). All of the ions are soluble in dmf and CH_3CN. The colors of the ions range from green for $[MoAs_8]^{2-}$(**2**), $[CrAs_8]^{3-}$ (**3**) and $[KCrAs_8]^{2-}$ (**4**) to red for $[MoSb_8]^{3-}$ (**5**). The crystals and their solutions are very air and moisture sensitive. Complexes **3**, **4**, and **5** are formally d^1 systems and rare examples of paramagnetic Zintl ion transition metal complexes. The complexes and their salts have been characterized by UV−vis spectroscopy, EPR, cyclic voltammetry, magnetic susceptibility, electrospray mass spectrometry (ESI−MS) and single-crystal X-ray diffraction.

Solid State Structures. There are two general structure types for the $[A(2,2,2\text{-crypt})]^+$ salts of the ME_8^{n-} ions; namely, free $[ME_8]^{n-}$ ions and 1D $[AME_8]^{n-}$ chains (M = Cr, Mo; E = As, Sb; A = alkali ion). Each of the complexes has different space groups and cell contents. A summary of the crystallographic data for **2**−**5** is given in Table 1, and the selected bond distances and angles are given in Table 2. A summary of the average metric parameters can be found in Table 3. The $[K(2,2,2\text{-crypt})]^+$ salt of **4** is tetragonal, space group *P*4/*ncc*, and is isomorphic to von Schnering's $[Rb(2,2,2\text{-crypt})]^+$ salt of $[RbNbAs_8]^{2-}$. The $[A(2,2,2\text{-crypt})]^+$ salts of **2**, **3** and **5** have monoclinic and triclinic structures.

The ME_8^{n-} ions have D_{4d} point symmetry with crown-like E_8 rings and interstitial transition metal atoms. In the salts of **2**,

(9) DiMaio, A. J.; Rheingold, A. L. *Chem. Rev.* **1990**, *90*, 169.
(10) Sullivan, P. J.; Rheingold, A. L. *Organometallics* **1982**, *1*, 1547.
(11) Rheingold, A. L.; Fountain, M. E.; DiMaio, A. J. *J. Am. Chem. Soc.* **1987**, *109*, 141.
(12) von Hanisch, C.; Fenske, D. *Z. Anorg. Allg. Chem.* **1997**, *623*, 1040.
(13) Scherer, O. J. *Angew. Chem., Int. Ed. Engl.* **1985**, *24*, 924.
(14) Scherer, O. J. *Angew. Chem., Int. Ed. Engl.* **1990**, *29*, 1104.
(15) Rheingold, A. L.; Foley, M. J.; Sullivan, P. J. *J. Am. Chem. Soc.* **1982**, *104*, 4727.
(16) Scherer, O. J.; Winter, R.; Heckmann, G.; Wolmershauser, G. *Angew. Chem., Int. Ed. Engl.* **1991**, *30*, 850.
(17) von Schnering, H. G. *Angew. Chem., Int. Ed. Engl.* **1981**, *20*, 33.
(18) Elmes, P. S.; Gatehouse, B. M.; Lloyd, D. J.; West, B. O. *J. Chem. Soc., Chem. Commun.* **1974**, 953.
(19) Issleib, K.; Hamann, B.; Schmidt, L. *Z. Anorg. Allg. Chem.* **1965**, *339*, 298.
(20) Breunig, H. J. *Z. Naturforsch. B* **1978**, *33*, 242.
(21) Mundt, O.; Becker, G.; Wessely, H.-J.; Breunig, H. J.; Kischkel, H. *Z. Anorg. Allg. Chem.* **1982**, *486*, 70.
(22) Breunig, H. J.; Soltani-Neshan, A. *J. Organomet. Chem.* **1984**, *262*, C27.
(23) Breunig, H. J.; Rosler, R.; Lork, E. *Angew. Chem., Int. Ed. Engl.* **1997**, *36*, 2237.
(24) Balazs, G.; Breunig, H. J.; Lork, E.; Mason, S. *Organometallics* **2003**, *22*, 576.
(25) Breunig, H. J.; Haberle, K.; Drager, M.; Severengiz, T. *Angew. Chem., Int. Ed. Engl.* **1985**, *24*, 72.
(26) Adolphson, D. G.; Corbett, J. D.; Merryman, D. *J. Am. Chem. Soc.* **1976**, *98*, 7234.
(27) Critchlow, S. C.; Corbett, J. D. *Inorg. Chem.* **1984**, *23*, 770.
(28) Charles, S.; Eichhorn, B. W.; Rheingold, A. L.; Bott, S. G. *J. Am. Chem. Soc.* **1994**, *116*, 8077.
(29) Bolle, U.; Tremel, W. *J. Chem. Soc. Chem. Commun.* **1994**, 217.

Table 1. Crystallographic Data for the $[MoAs_8]^{2-}$, $[CrAs_8]^{3-}$, $[KCrAs_8]^{2-}$, and $[MoSb_8]^{3-}$ Salts

empirical formula	$C_{38}H_{80}As_8K_2MoN_6O_{12}$	$C_{54}H_{108}As_8CrN_6Na_3O_{18}$	$C_{38}H_{80}As_8CrK_3N_6O_{12}$	$C_{162}H_{324}K_9Mo_3N_{18}O_{54}Sb_{24}$
compound formula	$[K(crypt)]_2$**2**·en	$[Na(crypt)]_3$**3**	$[K(crypt)]_2$**4**·en	$[K(crypt)]_3$**5**
formula weight	1586.58	1849.79	1581.74	6950.11
T (K)	153(2)	193(2)	193(2)	193(2)
wavelength (Å)	0.71073	0.71073	0.71073	0.71073
crystal system	monoclinic	triclinic	tetragonal	monoclinic
space group	*C*2/*c*	P-1	*P*4/*ncc*	I2
unit cell dimensions				
a[Å]	23.925(3)	13.9526(5)	20.5782(11)	25.8992(10)
b[Å]	11.7373(11)	16.2725(5)	20.5782(11)	25.3671(10)
c[Å]	20.703(2)	16.4417(6)	14.7662(16)	380125(2)
α[°]	90	90.2330(10)	90	90
β[°]	92.288(9)	94.4800(10)	90	92.4090(10)
γ[°]	90	97.4030(10)	90	90
volume (Å^3)	5808.9(11)	3690.2(2)	6252.9(8)	25025(2)
Z	4	2	4	4
D_{calc} (g/cm^3)	1.814	1.665	1.680	1.845
abs coeff. (mm^{-1})	4.948	3.798	4.637	2.901
data/restraints/parameters	5116/2/300	16832/0/927	2755/1/155	38101/7/2146
goodness-of-fit on F^2	0.995	1.031	1.132	0.987
final R indices [$I > 2\sigma(I)$][a]				
R1	0.0692	0.0346	0.0402	0.0548
wR2	0.1650 [3106 data]	0.0883 [12790 data]	0.1032 [2216 data]	0.1285 [26285 data]
R indices (all data)				
R1	0.0533	0.0947	0.0561	0.0951
wR2	0.1974	0.1226	0.1118	0.1443
largest peak/hole (eÅ^{-3})	1.469 and −1.009	1.229 and −0.401	0.742 and −0.567	2.071 and −0.779

[a] The function minimized during the full-matrix least-squares refinement was $R1 = \Sigma|F_o - F_c|/\Sigma F_o$, $wR2 = (\Sigma w|F_o)^2 - (F_c)^2|^2/\Sigma wF_o^2)^{1/2}$.

3, and **5,** the ME_8^{n-} ions are well separated from the cations, solvates and each other in their respective crystal lattices and are termed "free ions". In contrast, the noncryptated K^+ ions in **4** link the $CrAs_8^{3-}$ clusters into one-dimensional chains. ORTEP drawings of $[MoSb_8]^{3-}$ ions and the $[KCrAs_8]^{2-}$ 1D chain are given in Figures 1 and 2 as examples of the free-ion structures and the 1D chain structures, respectively. A common numbering scheme is used for all of the ME_8 units. Both complexes **2** and **4** have one en solvate molecule in their crystal lattices whereas **3** and **5** are solvate-free. There are three independent $[MoSb_8]^{3-}$ and nine $[K(2,2,2\text{-crypt})]^+$ ions in the asymmetric unit cell of the $[K(2,2,2\text{-crypt})]_3[MoSb_8]$ salt whereas the other crystals have only one unique ME_8 unit in their respective structures.

The general structures of the ME_8 units are highly symmetrical and show small systematic changes as M and E vary. The E−E distances within the respective As_8 and Sb_8 rings are almost the same within the experimental error (see Table 3). The transition metals are symmetrically coordinated to all of the eight atoms in the E_8 rings. These and subsequent studies will show that the E_8^{8-} rings are versatile ligands that can expand or contract in an accordion-like fashion by varying their E−E−E bond angles to accommodate various sizes of ions. As the size of the transition metal becomes smaller, the M−E distances necessarily become shorter which requires compression of the E−E−E angles (see Table 3). This puckering of the E_8 ring allows the E−E separations to remain at their optimal bond distance. These trends will become more apparent with the data from subsequent studies.[30]

The eight Mo−As distances in **2** average 2.563(2) Å, whereas the average Cr−As distances in **3** and **4** are only slightly shorter at 2.540(5) Å and 2.532(6) Å, respectively. The sum of the covalent radii of Mo−As and Cr−As are 2.59 Å and 2.48 Å, respectively.[31] These data suggest that the Cr atom is only loosely coordinated in the As_8 ring. The average As−As bond distances in **2**, **3**, and **4**, are 2.429(2) Å, 2.426(5) Å and 2.418(7) Å, respectively. The average Mo−Sb distance in **5** is 2.825(2) Å, which is quite similar to the sum of the covalent radii of Mo−Sb (2.80 Å).[31] The Sb−Sb distances in **5** average 2.786(2) Å and are approximately 0.36 Å longer on average than the corresponding As−As bonds in **2,** which is consistent with the differences in the covalent radii.

The bond angles in the As_8 ring are 90.6(2)° in the Mo complex **2** and decrease to 89.5(2)° in **3** to accommodate the smaller size of the Cr atom. As expected, the bond angles in the Sb_8 ring of $[MoSb_8]^{3-}$ are even more acute (85.0(2)°) relative to those of $[MoAs_8]^{2-}$ due to the increase in the size of the pnictide and the natural decrease in hybridization found for the heavier main-group elements. For example, a similar trend is observed in the Q_8 series[32−34] (Q = S, Se, Te) where the average E_8 bond angles progressively decrease from 108.2(6)° to 105.7(16)° to 100.0 (16)° for S_8, Se_8, and Te_8, respectively. For comparison, in the compounds containing neutral As_8 units, the As−As−As bond angles are 99.2° and 106.3(3)° for $(PhAs)_8Mo_2(CO)_6$ (ref 11) and 107.9(1)°, 99.1(1)°, and 96.9(1)° for $[(Cp''Nb)_2(\mu,\eta^{4:4}\text{−}As_8)]$ (ref 16). In the $(C_6H_5Sb)_6$·(1,4-dioxane) compound,[25] the Sb−Sb−Sb bond angles range from 86.8(1)° to 93.6(1)°. By comparison, the E−E−E bond angles in the $[ME_8]^{n-}$ complexes are compressed relative to the noncentered E_8 complexes just described. The compression presumably results from the optimization of M−E bonding at the expense of E_8 ring strain. It is interesting to note that we have not been able to isolate a $[CrSb_8]^{n-}$ ion to date. To accommodate a smaller atom (Cr), the Sb_8 ring would presumably need unreasonably acute E−E−E angles generating a highly strained complex.

(30) Kesanli, B.; Fettinger, J.; Scott, B.; Eichhorn, B., to be published.
(31) Greenwood, N. N.; Earnshaw, A. In *Chemistry of Elements*; Pergamon Press: Oxford, 1984; p 642 and 1170.
(32) Rettig, S. J.; Trotter, J. *Acta Crystallogr. Sect. C* **1987**, *43*, 2260.
(33) Cherin, P.; Unger, P. *Acta Crystallogr. Sect. B* **1972**, *28*, 313.
(34) Sheldrick, W. S.; Wachhold, M. *Angew. Chem., Intl. Ed. Engl.* **1995**, *34*, 450.

Table 2. Selected Bond Distances and Bond Angles of $[MoAs_8]^{2-}$, $[CrAs_8]^{3-}$, $[KCrAs_8]^{2-}$, and $[MoSb_8]^{3-}$ Ions

	distances			
	$[MoAs_8]^{2-}$	$[CrAs_8]^{3-}$	$[KCrAs_8]^{2-}$	$[MoSb_8]^{3-}$
M−E(1)	2.5694(12)	2.5230(6)	2.5384(6)	2.8255(15)
M−E(2)	2.5678(13)	2.5650(6)	2.5253(6)	2.8261(10)
M−E(3)	2.5637(15)	2.5346(6)	2.5384(6)	2.8248(11)
M−E(4)	2.5637(15)	2.5376(5)	2.5253(6)	2.8247(16)
M−E(5)	2.5678(13)	2.5295(5)	2.5384(6)	2.8247(16)
M−E(6)	2.5694(12)	2.5607(6)	2.5253(6)	2.8248(11)
M−E(7)	2.5686(15)	2.5348(5)	2.5384(6)	2.8261(10)
M−E(8)	2.5681(15)	2.5385(5)	2.5253(6)	2.8255(15)
E(1)−E(2)	2.4255(16)	2.4296(5)	2.4184(7)	2.7798(12)
E(2)−E(3)	2.4233(17)	2.4394(5)	2.4181(7)	2.7805(14)
E(3)−E(4)	2.432(3)	2.4261(5)	2.4184(7)	2.7935(16)
E(4)−E(5)	2.4233(17)	2.4179(4)	2.4181(7)	2.781(3)
E(5)−E(6)	2.4255(16)	2.4238(5)	2.4184(7)	2.7935(16)
E(6)−E(7)	2.4289(16)	2.4205(4)	2.4181(7)	2.7805(14)
E(7)−E(8)	2.437(3)	2.4221(4)	2.4184(7)	2.7798(12)
E(8)−E(1)	2.4289(16)	2.4243(5)	2.4181(7)	2.7971(17)

	angles		
E = As	$[MoAs_8]^{2-}$	$[CrAs_8]^{3-}$	$[KCrAs_8]^{2-}$
E(1)−E(2)−E(3)	90.94(5)	87.98(2)	89.89(3)
E(2)−E(3)−E(4)	90.60(6)	89.12(2)	89.12(3)
E(3)−E(4)−E(5)	90.60(6)	89.13(2)	89.89(3)
E(4)−E(5)−E(6)	90.94(5)	91.61(2)	89.12(3)
E(5)−E(6)−E(7)	91.19(6)	89.21(2)	89.89(3)
E(6)−E(7)−E(8)	91.14(6)	89.68(2)	89.12(3)
E(7)−E(8)−E(1)	91.14(6)	88.91(2)	89.89(3)
E(8)−E(1)−E(2)	91.19(6)	90.94(2)	89.12(3)

E = Sb	$[MoSb_8]^{3-}$
E(1)−E(2)−E(3)	84.98(6)
E(2)−E(3)−E(4)	85.25(4)
E(3)−E(4)−E(5)	84.92(6)
E(4)−E(5)−E(6)	84.92(6)
E(5)−E(6)−E(7)	85.25(4)
E(6)−E(7)−E(8)	84.98(6)
E(7)−E(8)−E(1)	84.73(4)
E(8)−E(1)−E(2)	84.73(4)

Table 3. Average Bond Distances (Å) and Angles (°) for the $[ME_8]^{n-}$ Ions

$[ME_8]^{n-}$	M–E	E–E	E–E–E
$[MoAs_8]^{2-}$	2.563(2)	2.429(2)	90.60(6)
$[CrAs_8]^{3-}$	2.540(5)	2.426(5)	89.54(16)
$[KCrAs_8]^{2-}$	2.532(6)	2.418(7)	89.50(3)
$[MoSb_8]^{3-}$	2.825(2)	2.786(2)	85.05(4)

The structure of the 1D chain complex, **4**, is made up of $CrAs_8$ units coordinated to K^+ ions to form a 1D chain propagating along the crystallographic *c*-axis (see Figure 2). The $[K(2,2,2\text{-crypt})]^+$ cations form a remarkable tetragonal array of channels that are alternately filled with chains of $[KCrAs_8]^{2-}$ ions and disordered en solvate molecules (see Figure 3). The structure of **4** is isomorphic to **1** except there are no solvate molecules located in the channels of the latter. Therefore, half of the channels in **1** are presumably empty and the remaining half contain the $[RbNbAs_8]^{2-}$ chains. It is likely that complex **1** also contains solvate molecules that could not be located due to extensive disorder. Because the solvent molecules of **4** are confined in the channels, they do not interact with the $[KCrAs_8]^{2-}$ ions but do form hydrogen bonds to the $[K(2,2,2\text{-crypt})]^+$ cations through the cryptand nitrogens. The $[CrAs_8]^{3-}$ units are staggered by 45° down the *c*-axis and bind to the K^+ ions in an η^4 fashion forming a square antiprismatic coordination environment. The nonbonding Cr−K separations along the chain axis are 3.692(2) (av) Å. The K−As contacts in the chain average 3.776(2) Å. The corresponding Rb−Nb and Rb−As distances in the isomorphic chain complex, **1**, are slightly longer at 3.76 Å and 3.92 Å, respectively.

It is interesting to note that the 1D chain complex, **4** forms in the presence of excess 2,2,2-crypt. Although solution studies on related compounds show that the absolute binding affinity of 2,2,2-crypt exceeds the $[ME_8]^{n-}$ complexes,[30] the formation of **4** under these conditions suggests that the alkali ion binding affinity of **4** is competitive with 2,2,2-crypt.

Electronic Structures and Electronic Spectra. The electronic structures of the hypothetical class of ME_8^{n-} ions (M = group 4−7, E = P, As, Sb) has been reported by Li and Wu.[8] Their results are summarized in Figure 4. The electronic absorption data for compounds **2**−**5** are listed in Table 4. The molecular orbital analysis can be used as an aid in assigning the transitions in these complexes.[8] All complexes show intense ligand-to-metal charge-transfer bands ($\epsilon > 1000$ $Lmol^{-1}cm^{-1}$) at high energies ($\lambda_{max} \approx 320$ nm). Although, the highest energy transition is almost the same for complexes **4** and **3** ($\lambda_{max} \approx 322$ nm), there is an increase in molar absorptivity coefficient from 10^3 to 10^4, respectively.

The electronic structure of the d^0 ME_8^{n-} complexes suggests that the low energy absorption for $[MoAs_8]^{2-}$ should be a $^1A_1 \rightarrow {}^1E_1$ transition possessing significant charge-transfer character. The MO diagram shows that the HOMO, ($9e_1$), is essentially As_8 lone pairs and the LUMO, ($8a_1$), is primarily the empty d_{z2} orbital of Mo. It is tempting to assign the band at 732 nm for **2** to this transition but the isoelectronic $[NbAs_8]^{3-}$ does not have an absorption in this region.[30] Assuming that the orbital orderings from Figure 4 are valid for the d^1 systems as well, the HOMO of the d^1 complexes should be a singly occupied d_{z2} orbital which gives rise to a $^2A_1$ ground state. EPR experiments suggest that this assumption may indeed be correct (see next section). Therefore, the lowest energy transitions for these complexes should be additional charge-transfer bands (i.e., $^2A_1 \rightarrow {}^2B_2$ or $^2A_1 \rightarrow {}^2E$). The absorptions at 780−790 nm for **3** and **4** are consistent with the charge-transfer transitions but once again, the absence of similar bands in the spectrum of the isoelectronic complex **5** precludes definitive assignments. Apparently, solvation effects and ion pairing significantly affect the electronic structures and absorption spectra of the ME_8^{n-} complexes, which makes assignments of the electronic transitions quite difficult.[35] Electronic correlations in the paramagnetic complexes further complicate the analysis of the electronic structures. Additional members of the ME_8^{n-} series coupled with more theoretical studies are necessary to make accurate assignments of the electronic spectra.

EPR. The room-temperature EPR spectra of the paramagnetic complexes were measured from dmf solutions (**3**−**5**) and CH_3CN solutions (**5**). The EPR spectra of **3** and **4** are virtually identical (Figure 5) and each show a signal at $g = 2.001$ with a 3.6 G hyperfine splitting due to coupling to all 8 atoms of the As_8 ring (^{75}As, I = 3/2, 100% abund.). The simulated pattern is in excellent agreement with the experimental spectrum (see inset, Figure 5). Hyperfine couplings to the Cr atoms were not resolved because of the low abundance of the ^{53}Cr isotope (^{53}Cr, I = 3/2, 9.6% abund.) relative to the abundance of spin-

(35) Li, J., personal communication, **2001**.

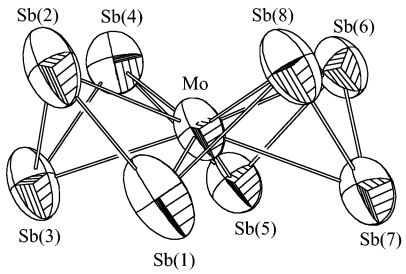

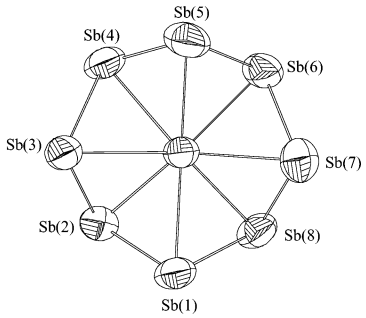

Figure 1. ORTEP drawings of the $MoSb_8^{3-}$ ion, **5**.

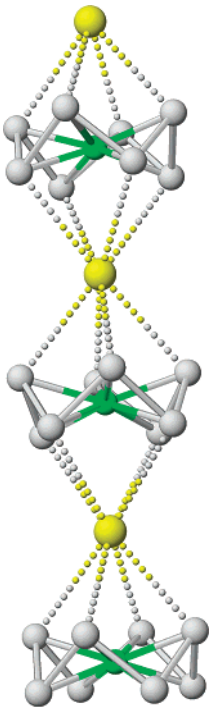

Figure 2. Ball-and-stick drawing of the $[KCrAs_8]^{2-}$ chain, **4**. As is gray, Cr is green, and K is yellow.

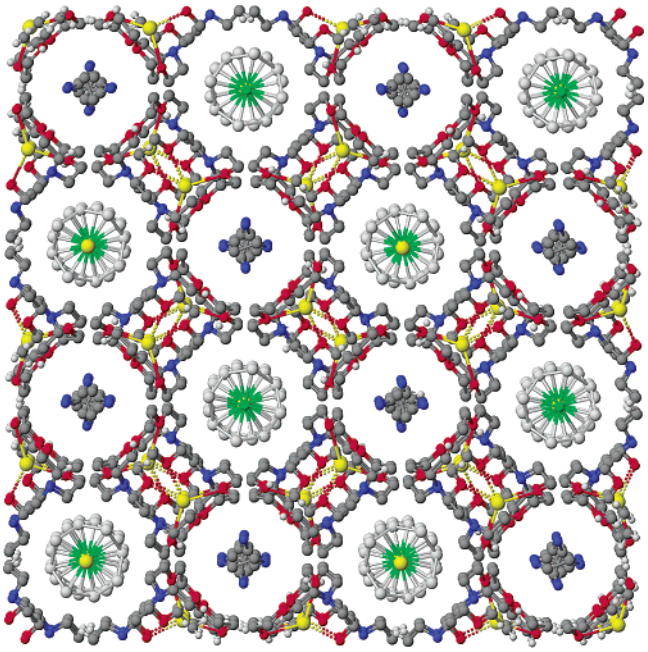

Figure 3. Projection of the $[K(2,2,2\text{-crypt})]_2[KCrAs_8]\cdot$en onto the a−b plane. The $[KCrAs_8]^{2-}$ units and disordered en molecules fill allternate channels in the structure. As is gray, Cr is green, K is yellow, carbon is dark gray, nitrogen blue, and oxygen red. The hydrogen atoms are omitted for clarity.

active As. For **5**, the EPR spectrum shows only a single broad resonance at g ≈ 1.86 with 150 G peak width and unresolved Sb and Mo hyperfine interactions in both dmf and CH_3CN. This resonance remains broad even when frozen at 78 K.

Assuming that the molecular orbital diagram of Li and Wu is valid for the paramagnetic d^1 systems, then the unpaired electron should be localized in a molecular orbital that is predominantly Cr d_{z2} in nature and contains only a small contribution from the As_8 ligand (Figure 4). From this analysis, one might anticipate that the EPR spectrum would show a large Cr hyperfine interaction with smaller couplings to the As_8 ring. Indeed, the ^{75}As hyperfine couplings of 3.6 G observed for **3** and **4** are significantly less than those reported values for As-centered radicals, which typically range from 30 to 1800 G.[36,37] The small hyperfine is consistent with a Cr-based radical but the associated Cr hyperfine cannot be resolved due to the low abundance of ^{53}Cr in the presence of eight ^{75}As nuclei. For comparison, the ^{53}Cr hyperfine coupling for $[Cr(N)(CN)_5]^{3-}$ is 24.9G,[38] which is typical for d^1 complexes.

Mass Spectrometry. The negative ion electrospray mass spectrum of $[K(2,2,2\text{-crypt})]_2[KCrAs_8]$ (dmf solution) shows mainly the oxidized molecular ion $[KCrAs_8]^{1-}$ together with the oxidized $[CrAs_8]^{1-}$ ion. The formation of oxidized and/or protonated molecular ions for Zintl polyanions in the ESI mass spectrum is typical[39] and multiply charged species have yet to be detected in any Zintl system. Labeling studies in related systems have shown that the protons originate from environmental sources and not the solvent. Various other As-containing cluster anions were also observed in the spectrum of **3**, such as $CrAs_9^{1-}$, As_8^{1-}, As_9^{1-}, As_{10}^{1-}, As_{12}^{1-}, As_{14}^{1-}, and As_{16}^{1-}. For the $[Na(2,2,2\text{-crypt})]_3[CrAs_8]$ salt, the ESI mass spectrum shows similar ions including the protonated and Na^+ coordinated ions (Figure 6). The dominant species however, are the oxidized $[CrAs_8]^{1-}$ ion and the Na^+ coordinated $[NaCrAs_8]^{1-}$ ion. The negative ion electrospray mass spectrum of **5** shows the oxidized molecular ion, $[MoSb_8]^{1-}$ and the K^+ coordinated $[KMoSb_8]^{1-}$ ion along with the $[MoSb_9]^{1-}$ ion. The spectrum

(36) Bagchi, R. N.; Bond, A. M.; Colton, R.; Creece, I.; McGregor, K.; Whyte, T. *Organometallics* **1991**, *10*, 2611.
(37) Morton, J. R.; Preston, K. F.; Strach, S. J. *J. Magn. Reson.* **1980**, *37*, 321.
(38) Bendix, J.; Deeth, R. J.; Weyhermuller, T.; Bill, E.; Wieghardt, K. *Inorg. Chem.* **2000**, *39*, 930.
(39) Kesanli, B.; Gardner, R. D.; Fettinger, J.; Eichhorn, B. *J. Am. Chem. Soc.* **2002**, *124*, 4779.

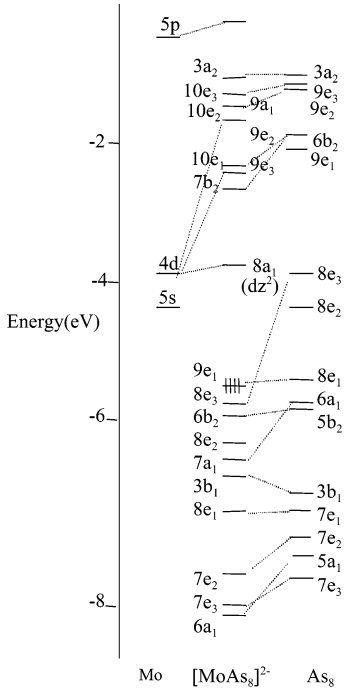

Figure 4. MO diagram of $[MoAs_8]^{2-}$ ion adapted from Li and Wu.[8]

Table 4. Electronic Absorption Data for the $[MoAs_8]^{2-}$, $[CrAs_8]^{3-}$, $[KCrAs_8]^{2-}$, and $[MoSb_8]^{3-}$ Ions.

	λ (nm)	ϵ ($Lmol^{-1}cm^{-1}$)
$[MoSb_8]^{3-}$	288	2.0×10^4
	362	1.7×10^4
	461	6.2×10^3
	508	4×10^3
$[MoAs_8]^{2-}$	384	2.4×10^3
	590	500
	670	1.0×10^3
	732	1.0×10^3
$[KCrAs_8]^{2-}$	322	1.2×10^3
	366	1.0×10^3
	583	475
	782	120
$[CrAs_8]^{3-}$	325	1.0×10^4
	445	3.4×10^3
	790	900

of **2** was reported earlier and shows the oxidized molecular ion $[MoAs_8]^{1-}$ and the K coordinated $[KMoAs_8]^{1-}$ ion as the main species.[7]

During the gas-phase studies of $[ME_8]^{n-}$ type complexes, the ubiquitous E_9 and ME_9 clusters are always observed. The E_9 ion appears to have a -3 charge as the $K_2E_9^{1-}$ ion has been observed in the mass spectra of related complexes.[30] The structure of the E_9 clusters and their metalated complexes, ME_9, are unknown.

Cyclic Voltammetry. Electrochemical studies for all complexes were conducted at room temperature from 1.5 mM dmf solutions containing 0.15M Bu_4PBr supporting electrolyte. The cyclic voltammogram of **2** (Figure 7) shows only a reversible one-electron oxidation at $-2.1V(\Delta E_{peak} = 0.12V)$ at scan rate 100mV/s. The cyclic voltammograms of **3** and **4** are virtually identical and also show a reversible single-electron oxidation similar to **2**. However the oxidation potential is shifted to a more positive potential at $-1.8V(\Delta E_{peak} = 0.11V)$ (Figure 7). No other waves were observed in the solvent window.

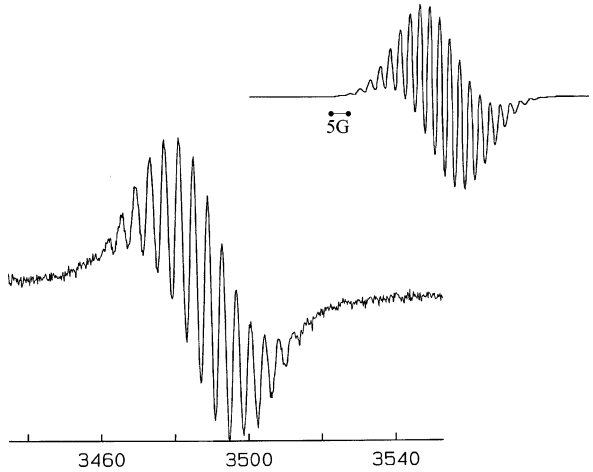

Figure 5. EPR Spectrum for $[KCrAs_8]^{2-}$ ion recorded from dmf solutions at 25 °C. The simulated spectrum is given in the inset.

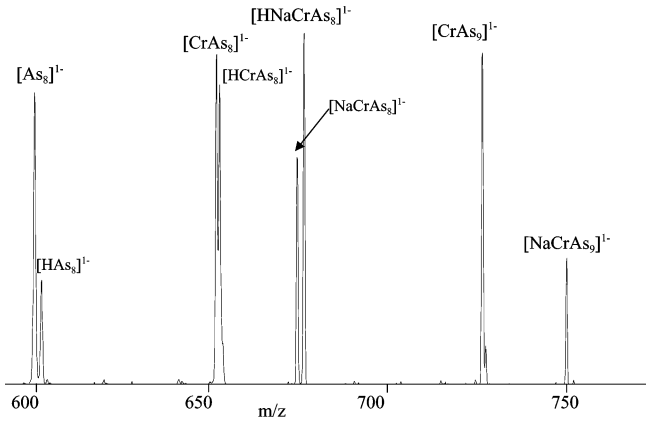

Figure 6. Electrospray mass spectrum (negative mode) of $[Na(2,2,2\text{-crypt})]_3[CrAs_8]$ recorded from dmf solution.

Complex **5** shows an ill-defined irreversible oxidation centered at ~ -2.3 V.

Magnetic Properties. The magnetic susceptibility of the $[K(2,2,2\text{-crypt})]_2[KCrAs_8]\cdot$en salt was measured from 300 to 5 K at a field of 5000 Oe. The diamagnetic correction[40] for the salt is 7.6×10^{-4} emu/mol and is significant at high temperatures where the measured susceptibility is $\sim 10^{-3}$ emu/mol. Calculation of the effective magnetic moment from the corrected data according to the formula

$$\mu_{eff} = \sqrt{\frac{3k_B T \chi_m}{N}}$$

revealed a μ_{eff} of $1.7\mu_B$ at high temperatures, which is consistent with a spin-1/2 system and indicates that the diamagnetic correction is reasonable. However, the plot of inverse susceptibility versus temperature (Figure 8a, inset) shows nonlinear paramagnetic behavior that does not obey the Curie−Weiss Law at low temperatures. A fit of the corrected susceptibility data above 150 K to the Curie−Weiss law

$$\chi_m = \frac{C}{T - \theta}$$

shows antiferromagnetic interactions with $C = 0.44$ emuK/mol

(40) O'Connor, C. H. *Prog. Inorg. Chem.* **1982**, *29*, 203.

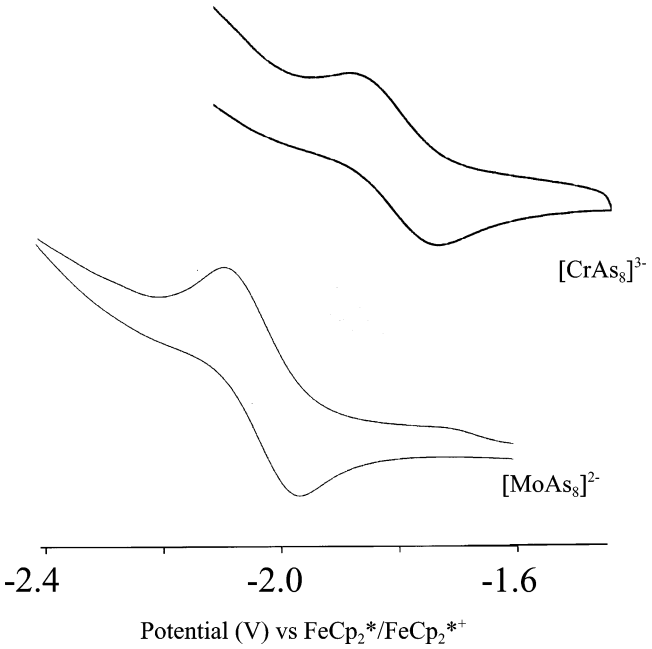

Figure 7. Cyclic voltammograms of $[MoAs_8]^{2-}$ (**2**) and $[CrAs_8]^{3-}$ (**3**) ions in dmf.

and $\theta = -35$ K (Figure 8a). The value of μ_{eff} decreases as the temperature is lowered and reaches a minimum value of $1.3\mu_B$ at 5 K (Figure 8b). To determine if the suppressed moment is due to antiferromagnetic coupling along the 1D $KCrAs_8^{2-}$ chains, the data were treated as a linear chain Heisenberg antiferromagnet (LCHA) in which the susceptibility is described by the formula[41]

$$\chi_m = \frac{Ng^2\mu_B^2}{k_BT}\left[\frac{0.25 + 0.14995y + 0.30094y^2}{1 + 1.9862y + 0.68854y^2 + 6.0626y^3}\right]$$

where $y = J/k_BT$, g is determined from EPR studies and k_B, N and μ_B are constants.[42] The value of J/k_B was estimated by fitting χ_m values to the above equation where the difference between the experimental and theoretical χ_m was minimized. The fit of the data to this model is shown in Figure 8a and reveals a small $-J/k_B$ of 3 K. These weak, one-dimensional interactions are similar to those observed for the weakly interacting electrides and alkalides reported by Dye and co-workers in related cryptate lattices.[43,44]

The susceptibility of the $[Na(crypt)]^+$ "free ion" salt of $CrAs_8^{3-}$ showed Curie−Weiss behavior to 5 K with $\theta \approx 0$ K (Figure 8c). The calculation of the magnetic moment was also complicated by the very large diamagnetic correction (1×10^{-3} emu/mol) which is approximately equal to the sample's susceptiblility ($\sim 1.5 \times 10^{-3}$ emu/mol) at high temperatures. The calculated moment of 1.3 μ_B is lower than expected. The deviation from a spin-only moment is presumably due to the large diamagnetic correction or a partial oxidation of the sample during the transfer to the SQUID magnetometer. However, the Curie−Weiss behavior is consistent with a diluted noninteracting paramagnetic spin system and is consistent with the free-ion structure. The large diamagnetic corrections necessary for the high formula mass of these compounds give rise to uncertainties in the measured moment in both compounds.

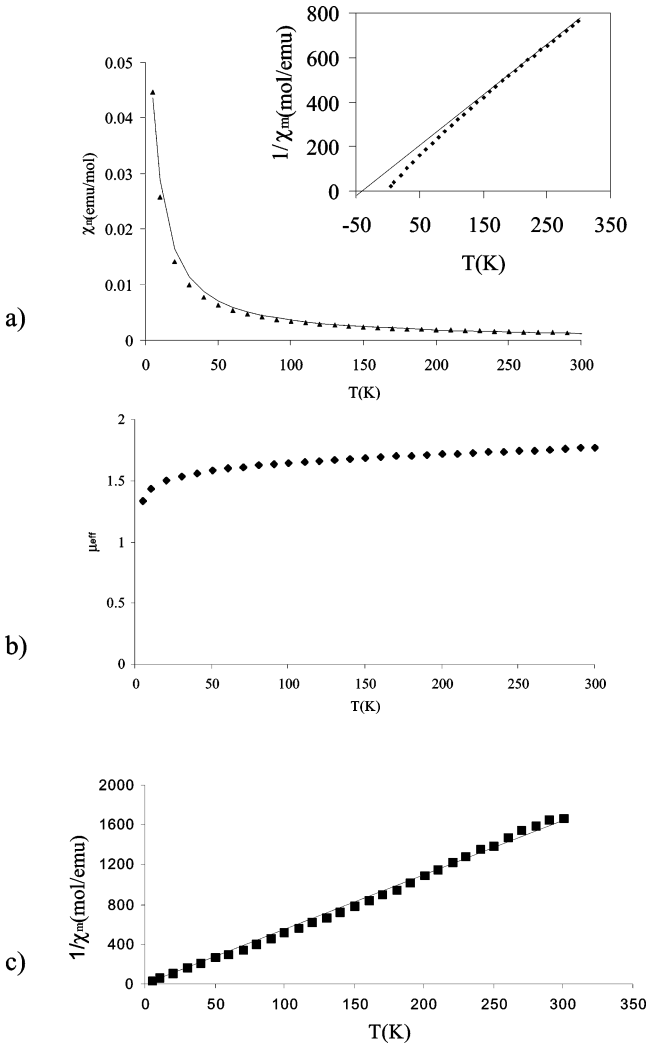

Figure 8. Plots of (a) magnetic susceptibility versus temperature for $[K(2,2,2\text{-crypt})]_2[KCrAs_8]$ at 5000 Oe field. The solid line shows the fit to the LCHA eqn (see text). The inset shows the reciprocal susceptibility and the fit of the high-temperature data to the CW eq (b) Effective magnetic moment versus temperature. (c) Reciprocal susceptibility for $[Na(2,2,2\text{-crypt})]_3[CrAs_8]$. The solid line represents a linear fit to the CW eqn. (see text).

Discussion

The E_8^{8-} rings in the ME_8^{n-} type ions are isoelectronic and isostructural to cyclooctane and the Q_8 molecules, S_8,[32] Se_8,[33] and Te_8 (in structure of Cs_3Te_{22}).[34] However, the Q_8 chalcogenides do not form MQ_8 type interstitial complexes. Instead, S_8 forms molecular adducts such as $WCl_6 \cdot S_8$, which contain alternating layers of neutral S_8 rings and WCl_6 molecules.[45] The ME_8^{n-} structure type is thus far unique to the pnictides but seems to represent a fairly generic class of complex ions. Attempts to extend the chemistry to include the P_8 derivatives and other transition metals is ongoing.

The mechanism of formation of the ME_8^{n-} type compounds is unknown. Much of the known chemistry of the Group 15

(41) Estes, W. E.; Gavel, D. P.; Hatfield, W. E.; Hodgson, D. J. *Inorg. Chem.* **1978**, *17*, 1415.
(42) Carlin, R. L. *Magnetochemistry*; Springer-Verlag: Berlin, 1986.
(43) Xie, Q. S.; Huang, R. H.; Ichimura, A. S.; Phillips, R. C.; Pratt, W. P.; Dye, J. L. *J. Am. Chem. Soc.* **2000**, *122*, 6971.
(44) Dye, J. L. *Inorg. Chem.* **1997**, *36*, 3816.
(45) Cotton, F. A.; Kibala, P. A.; Sandon, R. B. W. *Acta Crystallogr. Sect. C* **1989**, *45*, 1287.

Scheme 2

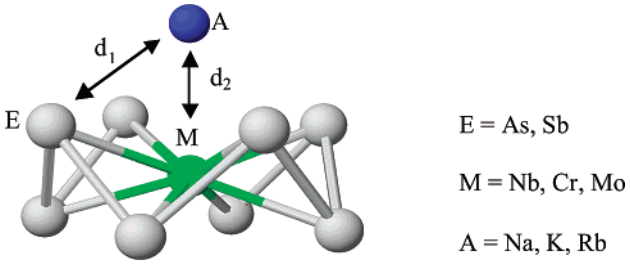

E_7^{3-} Zintl ions with transition metals involves the use of M(arene)$(CO)_3$ type precursors that yield compounds having CO ligands.[28,46] In all of these reactions, the number of atoms in the Zintl ion is always retained although the structure of the bare Zintl ion frequently rearranges.[47,48] The formation of E_8 (E = As, Sb) crown structures from the nortricyclane-like E_7 precursors requires reorganization of E−E bonds and cluster fragmentation and/or incorporation of additional pnictide atoms. The gas-phase studies of both Na_3As_7 and K_3As_7 parent alloys show predominately the As_7^{1-} ion together with trace amounts of As_8^{1-} and As_9^{1-} ions. Even though the As_8^{1-} ion is observed in the gas phase, it is significantly less abundant (<5 mol % of total As_n anions) than the parent As_7 species (~90 mol %) and is not present in sufficient concentrations to account for the relatively high yields of ME_8^{n-}complexes (20−45% yields based on As_7). Therefore, the formation of the ME_8^{n-} ions appears to be metal mediated. There are several possible mechanisms that could account for the conversion of the As_7^{3-} ions to the As_8 complexes, including the following: (1) the initial formation of an MAs_7 type complex that subsequently disproportionates to give MAs_8^{n-} ions; (2) initial formation of an MAs_7 type complex that assimilates an As atom from unreacted As metal present in the parent alloy to give MAs_8^{n-} ions ; and (3) the direct insertion of a metal atom (M) into a preformed As_8^{n-} ion that is generated from an equilibrium between As_7 and As_8 ions in solution. A study of the phosphorus analogues may provide insight into the mechanism of formation by way of ^{31}P NMR studies and is currently in progress.

The formation of one-dimensional chains in the solid state (e.g., $[K(2,2,2\text{-crypt})]_2[KCrAs_8]\cdot en$) versus free ion structures (e.g., $[Na(2,2,2\text{-crypt})]_3[CrAs_8]$) is governed by a combination of steric effects and Coulombic repulsions. The steric factors involve the sizes of the alkali ion (A), the main group atom (E) and the transition metal (M) that make up the ME_8 unit. The metric parameters contributing to the bonding in ME_8 are outlined in Scheme 2. The distance d_2 is the separation between the alkali ion and the transition metal while d_1 is the A−E bond distance. Distance d_2 governs the degree of electrostatic repulsion between M^{n+} and the alkali ion, A^+.

One-dimensional chain formation occurs when A−E interactions are optimized (favorable d_1), whereas the destabilizing electrostatic repulsions between M^{n+} and A^+ (d_2) are minimized. The following examples illustrate the interplay between d_1 and d_2. If d_2 becomes too small, the coulombic repulsions between A and M destabilize the chain structure and free ions are formed instead. Chain formation is therefore favored for small E, small M and large A. For example, a small alkali must drop down into the E_8 ring in order to maintain optimal A−E bonding (optimal d_1) which increases the M−A coulombic repulsion (short d_2). For the $CrAs_8^{3-}$ system, Na^+ ions appear to be too small to link the $CrAs_8$ rings (i.e., d_2 is too small) whereas the larger K^+ ions promote 1D chain formation. The same scenario is found for the Rb^+ and K^+ salts of $NbAs_8^{3-}$.[4,30] Similarly, increasing the E_8 ring diameter also requires the alkali ion to drop down into the ring to optimize A−E bonding (optimal d_1) which increases the M−A coulombic repulsions (short d_2). As a result, all of the Sb_8 complexes prepared to date are free ions. Finally, increasing the size of the transition metal with all other parameters constant also increases the M−A coulombic repulsion and destabilizes chain formation. For example the K^+ salts of the MAs_8^{3-} ions (M = Cr, Nb) form chains for M = Cr but are free ions for M = Nb. It should be noted that chain formation in the solid state requires the alkali ion to bind to the ME_8^{n-} ion (or growing chain in the nucleated crystal) instead of 2,2,2-crypt in solution.

In addition to rationalizing the solid-state structures, the steric and coulombic considerations described above also account for the reactivity of the ME_8 complexes in solution and in the gas phase. We previously showed through ESI−MS studies that **2** selectively binds to larger alkali metals in the gas phase.[7] In a subsequent publication, we show that this selectivity is operative in the solid state, the gas phase and in solution.[30]

According to the Zintl−Klemm formalism,[5,6] the E_8 ring formally possesses a −8 charge which makes it isoelectronic to S_8. This formalism requires high transition metal oxidation states, namely M^{5+} and M^{6+}. Although partitioning the oxidation states according to the Zintl−Klemm formalism clearly does not reflect the true atomic charges (i.e., the complexes are much more covalent),[8] the model does provide insight into the differences between the various ions. Within the group 6 E_8 complexes, higher transition metal oxidation states are observed for Mo versus Cr (e.g., $[CrAs_8]^{3-}$; Cr^{5+} and $[MoAs_8]^{2-}$; Mo^{6+}). This trend is consistent with the tendency of the 4d metals to adopt higher oxidation states relative to the 3d analogues in the same ligand environment (cf., $MoCl_5$ and $CrCl_3$).[31] Similarly, higher transition metal oxidation states are stabilized with the more electronegative As_8 rings relative to the less electronegative Sb_8 rings (e.g., $[MoAs_8]^{2-}$; Mo^{6+} and $[MoSb_8]^{3-}$; Mo^{5+}). Again a similar trend exists with the metal halides where the more electronegative fluoride anion stabilizes higher oxidation state transition metal complexes relative to the less electronegative halides (cf., CrF_6 and $CrCl_3$).[31]

In the cyclic voltammetry studies, $[MoAs_8]^{2-}$ undergoes single, reversible one-electron oxidation in dmf to give the monoanion, $[MoAs_8]^{1-}$ (eq 1), which was also observed in ESI−MS studies.[7] Salts of **3** and **4** both have a single reversible oxidation waves to form the $[CrAs_8]^{2-}$ ion (eq 2). Even though complex **4** is a 1D chain in the solid state, it behaves as a free ion in solution and therefore has the same electrochemical characteristics as **3**. The $[MoSb_8]^{3-}$ complex **5** reveals an ill-defined oxidation that is apparently irreversible.

Comparison of the $E_{1/2}$ values for these complexes indicates that it is easier to oxidize the d^1 complexes, **3** and **4**, relative to the d^0 complex, **2**. This trend is expected because the oxidation

(46) Fritz, G.; Hoppe, K. D.; Honle, W.; Weber, D.; Mujica, C.; Manriquez, V.; von Schnering, H. G. *J. Organomet. Chem.* **1983**, *249*, 63.
(47) Charles, S.; Eichhorn, B. W.; Bott, S. G. *J. Am. Chem. Soc.* **1993**, *115*, 5837.
(48) Ahlrichs, R.; Fenske, D.; Fromm, K.; Krautscheid, H.; Krautscheid, U.; Treutler, O. *Chem. Eur. J.* **1996**, *2*, 238.

of **2** requires the formal oxidation of the As_8 ring as Mo is already in the highest valance state. In contrast, the Cr^{5+} (d^1) ion in **3** and **4** can be further oxidized to Cr^{6+} (d^0) without the formal oxidation of the As_8 ring. Surprisingly, there was no reduction of $[MoAs_8]^{2-}$ to form the putative d^1 complex, $[MoAs_8]^{3-}$, which is the most stable form of the closely related $[MoSb_8]^{3-}$ and $[CrAs_8]^{3-}$ complexes

$$MoAs_8^{2-} \rightleftarrows MoAs_8^{-} + e^- \quad E_{1/2}(V) = -2.1 \qquad (1)$$

$$CrAs_8^{3-} \rightleftarrows CrAs_8^{2-} + e^- \quad E_{1/2}(V) = -1.8 \qquad (2)$$

The electrochemical data are consistent with metal-based oxidations for **3** and **4** with a ligand-based oxidation for **2**. These findings support the electronic structures described by Li and Wu and are also consistent with the EPR data for the paramagnetic complexes.

Summary. We have shown that the E_8 ring is an unusual but versatile 8-coordinate ligand that forms 16-electron diamagnetic and 17-electron paramagnetic homoleptic ME_8^{n-} ions with group 5 and 6 transition metals. The accordion-like nature of the ring should allow for an extensive series of compounds with differing electronic configurations. The electrochemical and EPR properties of these compounds are consistent with the electronic structures of **2** described by Li and Wu.[8] The 16 electron compounds have arsenic-centered HOMO's with metal-based d_{z2} LUMO's. The unpaired electrons in the paramagnetic 17 electron complexes reside in the d_{z2} orbitals of the metal. Importantly, we have shown that by adjusting the steric properties of the alkali ion and the main group element, we can switch between free-ion structures and one-dimensional chains in the solid state. These factors can be used to ratonalize the formation of chain structures in the $[KCrAs_8]^{2-}$ and $[RbNbAs_8]^{2-}$ ions[4] and serve as a guide for designing chain or free ion structures in the future. The presence of magnetic coupling through the nonmagnetic alkali ions suggest that ferro or ferrimagnetic exchange may be induced if magnetic ions (e.g., Eu^{2+}) could be used to link the ME_8^{n-} ions. Further studies are in progress.

Experimental Section

General Data. All reactions were performed in a nitrogen filled drybox (Vacuum Atmospheres Company). The cyclic voltammetry studies were carried out with Bioanalytical Systems BAS-100a at 25 °C. The samples were prepared in a drybox and placed into an airtight three-electrode glass cell. The sample concentrations were 1.5mM with a supporting electrolyte (*n*-Bu_4PBr) concentration of 0.15M. A Pt working electrode, Ag/AgCl reference and Pt auxiliary electrode were used in the electrochemical measurements. Cyclic voltammograms were run at 100 and 500mV/s scan rates and referenced to an external decamethylferrocene standard (0.0 V). The $FeCp^*_2/FeCp^*_2{}^+$ couple, was employed as an external reference and showed a $\Delta E_{peak} = 0.11V$ under the experimental conditions employed here. A HP 8453 Spectrophotometer was used for electronic absorption spectra. A Bruker 200D-SRC EPR Spectrometer was used for the EPR analysis. Samples were drawn into 50 μL capillaries in a drybox and sealed at the top and bottom. The sealed capillaries were then placed within standard 3 mm internal diameter quartz EPR tubes. The *g* value was calculated by comparing the signal of the sample to the diphenylpicrylhydrazyl standard.[49] Electrospray mass spectra were recorded from dmf solutions on a Finnigan mass spectrometer by way of direct injection. The samples were ionized by using an ESI probe and detected in the negative ion mode. The D.C. magnetic susceptibilities were measured using a Quantum Design MPMS SQUID magnetometer by Dr. Serpil Gonen. Crystalline samples were loaded into a gelatin capsule and the field was applied (5000 Oe) after the sample was cooled to 5 K (ZFC, zero field cooled). The magnetization was measured as the sample was warmed.

Chemicals. Melts of nominal composition A_3E_7 (A = Na, K; E = As; A = K, E = Sb) were prepared by high-temperature fusion (~1000 °C) of stoichiometric ratios of the elements. The chemicals were sealed in evacuated, silica tubes and carefully heated with a natural gas/oxygen flame. **CAUTION:** Fusing alkali metals with pnictide elements is highly exothermic and can result in explosion. Preparations of the melts must be conducted behind blast shields and only small quantities (<2 g) should be prepared. Anhydrous ethylenediamine (en) and dimethylformamide (dmf) were purchased from Fisher, vacuum distilled from K_4Sn_9 and stored under dinitrogen. Toluene was distilled from sodium/benzophenone under dinitrogen and stored under dinitrogen. CH_3CN was purchased from Aldrich and distilled over CaH_2 and kept under dinitrogen. 4,7,13,16,21,24-hexaoxa-1,10-diazobicyclo[8.8.8] hexacosane (2,2,2-crypt) was purchased from Aldrich. Mo(Me-naphthalene)$_2$,[50] Mo(naphthalene)$_2$ and Cr(naphthalene)$_2$[51] were prepared according to the literature procedures. The synthesis of $[K(2,2,2\text{-crypt})]_2[MoAs_8]$ was previously reported.[7]

Synthesis. Preparation of $[K(2,2,2\text{-crypt})]_2[KCrAs_8]$.en. In vial 1, K_3As_7 (50.0 mg, 0.078 mmol) and 2,2,2-crypt (88.0 mg, 0.234 mmol) were dissolved in ca. 2 mL of en producing a dark red solution. In vial 2, Cr(naphthalene)$_2$ (24.0 mg, 0.078 mmol) was dissolved in warm toluene (ca. 1 mL) producing a violet solution. The contents of vial 2 were added to the contents of vial 1 yielding a green-brown solution. The reaction mixture was stirred overnight and filtered through tightly packed glass wool in a pipet. Toluene was added dropwise to the reaction mixture until precipitate formation was observed. The solution was filtered immediately. Green crystals formed in the reaction vessel after 24 h.Yield: 43 mg (35%).

Preparation of $[Na(2,2,2\text{-crypt})]_3[CrAs_8]$. In vial 1, Na_3As_7 (30.0 mg, 0.051 mmol) and 2,2,2-crypt (57.6 mg, 0.153 mmol) were dissolved in ca. 2 mL of en producing a brown-orange solution. In vial 2, Cr(naphthalene)$_2$ (15.7 mg, 0.051 mmol) was dissolved in warm toluene (ca. 1 mL) producing a violet solution. The contents of vial 2 were added to the contents of vial 1 yielding a green-brown solution. The reaction mixture was stirred overnight and filtered through tightly packed glass wool in a pipet. Toluene was added dropwise to the reaction mixture until precipitate formation was observed. The solution was then filtered immediately. Green crystals formed in the reaction vessel after 24 h. Yield: 32 mg (34%).

Preparation of $[K(2,2,2\text{-crypt})]_3[MoSb_8]$. In vial 1, K_3Sb_7 (50.0 mg, 0.052 mmol) and 2,2,2-crypt (58.8 mg, 0.156 mmol) were dissolved in ca. 2 mL of en producing a dark red/brown solution. In vial 2, Mo(Me-naphthalene)$_2$ (19.6 mg, 0.052 mmol) was dissolved in toluene (ca. 1 mL) producing a red-brown solution. The contents of vial 2 were added to the contents of vial 1 yielding a dark brown solution. The reaction mixture was stirred for 8 h and filtered through tightly packed glass wool in a pipet. Toluene was added dropwise to the reaction mixture until precipitate formation was observed. The solution was filtered immediately. Red crystals formed in the reaction vessel after 2 d. Yield: 18 mg (15%).

Preparation of $[K(2,2,2\text{-crypt})]_2[MoAs_8]$. In vial 1, K_3As_7 (50.0 mg, 0.078 mmol) and 2,2,2-crypt (88.0 mg, 0.234 mmol) were dissolved in ca. 2 mL of en producing a dark red solution. In vial 2, Mo(naphthalene)$_2$ (27.4 mg, 0.078 mmol) was dissolved in toluene (ca. 1 mL) producing a violet solution. The contents of vial 2 were added

(49) Ya, S. *EPR of Free Radicals*; Wiley: New York, 1974.

(50) Thi, N. P. D.; Spichiger, S.; Paglia, P.; Bernardinelli, G.; Kundig, E. P.; Timms, P. L. *Helv. Chim. Acta* **1992**, *75*, 2593.

(51) Pomije, M. K.; Kurth, C. J.; Ellis, J. E.; Barybin, M. V. *Organometallics* **1997**, *16*, 3582.

to the contents of vial 1 yielding a green-brown solution. The reaction mixture was stirred for 4 h and filtered through tightly packed glass wool in a pipet. Toluene was added dropwise to the reaction mixture until precipitate formation was observed. The solution was filtered immediately. Green crystals formed in the reaction vessel after 24h.Yield: 53 mg (45%). An alternative synthetic procedure using the $Mo(Me\text{-}naphthalene)_2$ precursor can be found in ref 7.

Crystallographic Studies. $[MoAs_8][K(crypt)]_2\cdot en$. A large irregular shaped green plate with dimensions 0.675 × 0.375 × 0.100 mm was placed and optically centered on the Enraf-Nonius CAD-4 diffractometer. The crystals' final cell parameters and crystal orientation matrix were determined from 25 reflections in the range $17.9 < \theta < 18.3°$; these constants were confirmed with axial photographs. Data were collected [MoKα] with ω scans over the range $1.7 < \theta < 25.0°$ with a scan width of $(1.15 + 0.55\tan\theta)°$ and variable scan speed of 3.3−4.1° min.$^{-1}$ with each scan recorded in 96 steps with the outermost 16 steps on each end of the scan being used for background determination. Minor variations in intensity were observed; data were not corrected. Seven ψ-scan reflections were collected over the theta range $7.8 < \theta < 12.1°$; the absorption correction was applied with transmission factors ranging from 0.0362 to 0.0939. Two forms of data were collected, Friedel pairs, indices $\pm h-k-l$ and $\pm hkl$; resulting in the measurement of 10 488 reflections; 5116 unique [R(int) = 0.0759].

Data were corrected for Lorentz and polarization factors and reduced to F_o^2 and $\sigma(F_o^2)$. Intensity statistics and systematic absences clearly indicated the centrosymmetric monoclinic space group $C2/c$ (no. 15). The structure was determined by direct methods (XS)[52] with the successful location of the $MoAs_8$ unit along with the potassium atom. Two difference Fourier map refinement cycles were required to locate all of the remaining non-hydrogen atoms comprising the $[K(crypt)]^+$ ion. The ethylenediamine molecule was disordered about an inversion center. The occupancies of the two orientations were fixed at 0.5 with the nitrogen thermal parameters constrained (EADP).[52] After several cycles of refinement, all of the non-hydrogen atoms comprising the $MoAs_8^{2-}$ and $[K(crypt)]^+$ ions were refined anisotropically. The atoms comprising the ethylenediamine produced wildly varying ellipsoids and were refined isotropically. Hydrogen atoms attached to carbon and nitrogen atoms were placed in calculated positions; these being dependent on both the type of bonding and the temperature (153(2)K in this case) with methylene $d(C-H_2) = 0.990$ Å, U_H equals $1.2U_{(parent)}$, and nitrogen $d(N-H_2) = 0.880$ Å with U_H equal to $1.2U_{(parent)}$. These hydrogen atom positions were updated after each stage of refinement but not allowed to refine freely. The structure was refined to convergence [$\Delta/\sigma \leq 0.001$]. A final difference Fourier map possessed many peaks with $|\Delta\rho| \geq 1.00$ e**Å**$^{-3}$, and as large as 1.47 e**Å**$^{-3}$, within 1.6**Å** of the atoms comprising the $MoAs_8$ molecule. The largest other extraneous peak had a $|\Delta\rho| = 0.82$ e**Å**$^{-3}$ and was within 0.56 **Å** of H42B indicating that the structure is both correct and complete.

$[KCrAs_8][K(crypt)]_2\cdot en$. A dark block with dimensions 0.673 × 0.42 × 0.237 mm^3 was placed and optically centered on the Bruker SMART CCD system at −80 °C. The initial unit cell was indexed using a least-squares analysis of a random set of reflections collected from three series of 0.3° wide ω scans (25 frames/series) that were well distributed in reciprocal space. Data frames were collected [MoKα] with 0.3° wide ω-scans for 40 s. Five complete ω-scan series, 606 frames, were collected with an additional 200 frames a repeat of the first series for redundancy and decay purposes. The crystal to detector distance was 4.930 cm, thus providing a complete sphere of data to $2\theta_{max}$=50.0°. A total of 44 205 reflections were corrected for Lorentz and polarization effects and absorption using Blessing's method as incorporated into the program SADABS.[53]

System symmetry and systematic absences indicated the unique centrosymmetric tetragonal space group *P4ncc* (no. 130). The 44205 data collected were merged based upon identical indices yielding 31 935 data [R(int) = 0.0652] which were further merged during least-squares refinement to 2755 unique data [R(int) = 0.1054]. The structure was determined by direct methods with the successful location of nearly all non-hydrogen atoms using the program XS.[52] After several refinement/difference Fourier cycles, nearly all of the atoms were refined isotropically and then anisotropically. The carbon and nitrogen atoms comprising the ethylenediamine molecule possessed very large thermal parameters and were therefore refined isotropically. Hydrogen atoms were placed in calculated positions. Several of the low angle reflections were unexpectedly large due most probably to twinning so a SHEL instruction was input to omit them. The final structure was refined to convergence [$\Delta/\sigma \leq 0.001$]. A final difference Fourier map was featureless indicating that the structure is therefore both correct and complete.

$[CrAs_8][Na(crypt)]_3$. A dark green block with dimensions 0.621 × 0.421 × 0.577 mm^3 was placed and optically centered on the Bruker SMART CCD system at −80 °C and processed as described above. A total of 58 657 reflections were collected and merged to 16 832 unique [R(int) = 0.0271]. The data indicated the triclinic space group P-1. The structure was solved by direct methods (XS)[52] and the refined to convergence as described above. The final difference map was essentially featureless with several small peaks near the $CrAs_8$ heavy atoms. See Table 1 for the crystallographic summary.

$[MoSb_8][K(crypt)]_3$. A very thin red plate with dimensions 0.461 × 0.334 × 0.014 mm^3 was placed and optically centered on the Bruker SMART CCD system at −80 °C and processed as described above. The data were consistent with either a monoclinic *C*-centered or monoclinic *I*-centered cell. Systematic absences and intensity statistics indicated either the chiral space group *I*2 (# 5), the centrosymmetric space group *I*2/*m* (# 12) or the acentric space group Im (# 8). Intensity statistics indicated *I*2 and, of attempted solutions in all three possible space groups, only *I*2 gave a direct methods solution (XS).[52] The structure was refined by the usual series of least squares difference Fourier cycles. The absolute structure parameter, Flack(x), refined to nearly 0.5 indicating racemic twinning. This problem was accommodated by a set of TWIN/BASF set of instructions. The final structure was refined to convergence [$\Delta/\sigma \leq 0.001$] yielding a final difference Fourier map with several peaks near the Sb atoms but was otherwise featureless. See Table 1 for the crystallographic summary.

Acknowledgment. We are very grateful to Dr. Serpil Gönen for help with the susceptibility measurements and for valuable discussions.

Supporting Information Available: Crystallographic files for **2**−**5** in .cif format. This material is available free of charge via the Internet at http://pubs.acs.org.

JA034207E

(52) Sheldrick, G. M.; SHELXTL version 5.03; Siemens Analytical X-ray Instruments, Inc.: Madison, WI, 1994.

(53) Sheldrick, G. M.; SADABS−Siemens Area Dectector Absorption Correction System; Universitat Gottingen: Gottingen, Germany, 1996.